scientific **data**

DATA DESCRIPTOR

Check for updates

High-resolution Digital Surface Model of the 2021 eruption deposit of Cumbre Vieja volcano, La Palma, Spain

Riccardo Civico [1] ✉, Tullio Ricci [1], Piergiorgio Scarlato [1], Jacopo Taddeucci [1], Daniele Andronico [2], Elisabetta Del Bello [1], Luca D'Auria [3,4], Pedro A. Hernández[3,4] & Nemesio M. Pérez[3,4]

Identifying accurate topographic variations associated with volcanic eruptions plays a key role in obtaining information on eruptive parameters, volcano structure, input data for volcano processes modelling, and civil protection and recovery actions. The 2021 eruption of Cumbre Vieja volcano is the largest eruptive event in the recorded history for La Palma Island. Over the course of almost 3 months, the volcano produced profound morphological changes in the landscape affecting both the natural and the anthropic environment over an area of tens of km². We present the results of a UAS (Unoccupied Aircraft System) survey consisting of >12,000 photographs coupled with Structure-from-Motion photogrammetry that allowed us to produce a very-high-resolution (0.2 m/pixel) Digital Surface Model (DSM). We characterised the surface topography of the newly formed volcanic landforms and produced an elevation difference map by differencing our survey and a pre-event surface, identifying morphological changes in detail. The present DSM, the first one with such a high resolution to our knowledge, represents a relevant contribution to both the scientific community and the local authorities.

Background & Summary

The morphology of active volcanoes is dynamically shaped by eruptive activity and erosional processes acting at different timescales. Consequently, a precise digital elevation model is fundamental for mapping volcanic hazards, modelling volcanic processes, and complementing further analysis. Furthermore, in urbanised areas, detailed post-eruption topography is important for land recovery actions. Volcano morphologies can be quantified using different techniques[1–9]. Recently, the increased capability of UASs and their applications for aerial observation[10,11], together with the parallel development of Structure-from-Motion (SfM) process[12], brought important and valuable advantages compared to the classical ground-based, satellite, and crewed aircraft surveys. Nowadays, UAS-based photogrammetry is routinely applied on volcanoes to obtain very-high-resolution DSMs[13–16].

Cumbre Vieja is the active volcanic rift on La Palma and has seen the largest number of eruptions of the Canary archipelago in historic times[17], and its 2021 eruption was the largest eruptive event in recorded history for La Palma. The previous eruption occurred in the southern part of the island between September and November 1971. The 2021 eruption was preceded by an unrest phase characterised by increased ground deformation starting from 2009[18], increased seismicity from 2017[19–22], and detection of geochemical anomalies from 2010[23]. A dramatic evolution of the seismicity began on 11 September 2021 with a seismic swarm characterised by an upward migration of the hypocentres reflecting the rising of magma towards the surface.

The volcanic eruption at Cumbre Vieja started on September 19, interrupting its 50-years-long period of quiescence, and lasted until December 13 (85 days and 8 hours[24]). During this period, the volcanic activity

[1]Istituto Nazionale di Geofisica e Vulcanologia, Roma, Italy. [2]Istituto Nazionale di Geofisica e Vulcanologia, Osservatorio Etneo, Catania, Italy. [3]Instituto Volcanológico de Canarias (INVOLCAN), San Cristóbal de La Laguna, Tenerife, Canary Islands, Spain. [4]Instituto Tecnológico y de Energías Renovables (ITER), Granadilla de Abona, Tenerife, Canary Islands, Spain. ✉e-mail: riccardo.civico@ingv.it

was distributed along a fissure where a multiple-vents volcanic edifice formed (called "Volcán de Tajogaite"). The explosive activity was characterised by alternating strombolian explosions and lava fountaining episodes, accompanied by abundant lava effusion. All such phenomena produced profound morphological changes in the landscape and severely affected settlements and industry. A total of about 12 km² of territory, more than 1,600 buildings and 200 hectares of banana plantations (the island's main economic resource after tourism), and important infrastructures (roads, powerlines, waterlines, etc.) were buried and destroyed by lava flows in their 6-km-long-path to the ocean. Here they expanded into two lava deltas, forming new land. In addition, the tephra fallout further affected the whole island and, to a smaller extent, the nearby islands of El Hierro, La Gomera and Tenerife.

Here, we present the results of a UAS survey carried out between 24 and 28 January 2022 using a DJI Phantom 4 RTK (real-time kinematic). The aerial images were georeferenced using an onboard RTK receiver capable of cm-level positioning accuracy. The dataset was then processed using Structure-from-Motion (SfM) photogrammetry and 40 Ground Control Points (GCPs) acquired between 23 and 27 January using the Differential Global Navigation Satellite System (DGNSS) positioning. This allowed us to achieve horizontal and vertical centimetre accuracy and to produce a very-high-resolution (0.2 m/pixel) Digital Surface Model (DSM) and orthophotomosaic (0.1 m/pixel), covering an area of about 17 km².

Topographic change detection was obtained by differencing our survey and a pre-event (2015) 2m-pixel DTM[25], thus identifying elevation changes at decimetre level precision. We characterised the whole topography of the new volcanic edifice and related lava field to detect elevation, areal, and volume variations.

Summary of the main findings:

- Subaerial deposit of lava flows and proximal fallout: volume 217.4 ± 6.6 Mm³ (voids in the lava field and submerged portion of the two deltas are not considered), subaerial deposition rate 29.5 m³/s. In a previous survey carried out on 27/9, 35.8 ± 3.0 Mm³ and 59.2 m³/s were recorded[26]. Moreover, considering the volume difference between the 27/09 survey[26] and the post-event survey, the resulting subaerial deposition rate is 27.2 m³/s.
- Volcanic edifice: volume 36.5 ± 0.3 Mm³ (8.9 ± 0.2 Mm³ on 27/9[26]); surface 0.6 km²; major and minor axes of the cone, calculated along the main eruptive fracture, approximately 770 (N 140°) and 660 m, respectively; maximum elevation difference 187 m; maximum height 1071.2 m a.s.l.
- Subaerial lava flows: volume 177.6 ± 5.8 Mm³ (including fallout deposit on lava flows); surface 11.8 km² (deltas 0.48 km²); maximum and average thickness 65 and 15.2 m, respectively; effusion rate 24.1 m³/s (submerged volume of lava deltas is not considered).

The present DSM represents a relevant contribution to both the scientific community and the authorities in charge of the restoration activities management.

Methods

UAS survey and DSM generation. We conducted a photographic survey campaign (Fig. 1 and Table 1) between 24 and 28 January 2022, collecting multiple sets of UAS-based high-resolution imagery. We acquired over 12000 aerial pictures using a DJI Phantom 4 RTK UAS with a 1" CMOS 20MP and a field of view (FOV) 84° and 8,8 mm/24 mm (35 mm equivalent) focal length lens.

A total of 10 multi-flight missions were conducted for the survey, for a cumulative flight path of over 800 km (Fig. 1). All flights except two were nadir image data collection missions, conducted at an approximate altitude of 200 metres above ground level (a.g.l.), resulting in a nominal ground-sampling-distance (GSD) of 5.4 centimetres per-pixel. The 24 and 28 January 2022 flights carried out in the area of the cone were both nadir and oblique image data collection missions conducted at a variable altitude of 50–200 metres a.g.l. For the nadir flights, we flew the UAS using predefined missions. Flight planning was designed with 80% forward and side overlap at ground level. Before each flight, we adjusted the camera's digital ISO, aperture, and shutter speed according to ambient light conditions.

With respect to other terrains, several additional difficulties characterised the aerial photographic survey campaign at Cumbre Vieja. The cone area has a highly irregular topography, characterised by notched craters and slopes. In addition, viewing conditions at Cumbre Vieja were still partially limited by the presence of vapour/gas plumes and, at times, by atmospheric haze and clouds.

The data on camera position were collected using GNSS-RTK information embedded in the image metadata by means of a DJI D-RTK 2 Mobile Station. In addition, 40 ground control points (GCPs) were distributed along the outer boundary of the lava flow and in the cone area to establish survey control (Fig. 1). In detail, 33 points were used as proper GCPs (i.e., used to georeference and scale the photogrammetric model and for camera calibration purposes), whereas 7 points were used as checkpoints (i.e., not directly used in the photogrammetric modelling process but available to check the accuracy of the generated model). GCPs were measured with a GNSS survey using a DJI D-RTK 2 Mobile Station in real-time kinematic (RTK) mode, with differential corrections sent in real-time by the Instituto Geográfico Nacional differential positioning service available at https://www.ign.es/web/ign/portal/gds-gnss-tiempo-real. The surveyed GCPs have an accuracy of 1–2 cm in horizontal coordinates and 2–4 cm in elevation.

Following image collection, we culled the photoset, removing dark and/or blurry photos. We then processed 9970 georeferenced images using the Agisoft Metashape® software package (version 1.6.3) based on the Structure-from-Motion and multi-view stereo photogrammetry algorithm (SfM–MVS)[12]. The workflow of our photogrammetric analysis included the following: (1) image masking for areas with strong degassing and/or unnecessary background; (2) camera triangulation with image position and orientation and generation of sparse point cloud; (3) filtering of the sparse point cloud to remove points with bad geometry, large pixel matching errors, and large pixel residual errors; (4) generation of the dense point cloud; (5) cleaning of the dense point
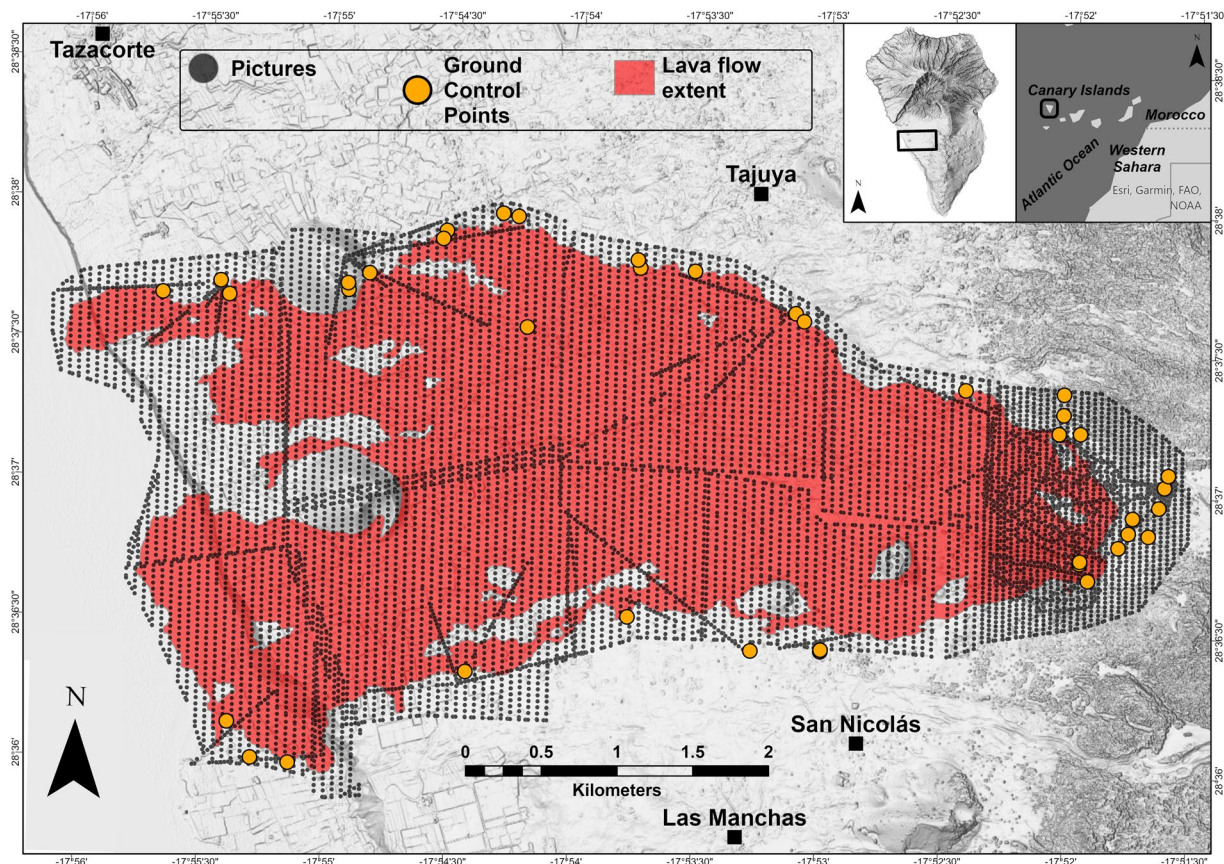
Fig. 1 Map identifying the location of each image acquired during the survey (grey dots) and the ground control points used to establish survey control (orange dots). Extent of the lava field (in red) as of 2021-12-18 - [EMSR546] - from Copernicus Emergency Management Service (© 2021 European Union[28]). The inset at the top right of the figure shows the location of La Palma island and the survey area.

Number of images	Camera stations	Flying altitude (m a.g.l.)	Ground resolution (cm/pixel)	Tie points	Projections
10,437	9,970	187	4.46	2,751,497	17,509,917
Reprojection error (pixel)	**Dense cloud points**	**DSM resolution (cm/pixel)**	**Point density (pts/m²)**	**DSM area (km²)**	
0.642	2,746,820,588	8.91	126	17.16	

**Table 1.** Details of the photogrammetric survey data and elaboration.

cloud by using the "filter by confidence" tool and by manually removing anomalous floating points caused by the presence of the volcanic plume; and (6) generation of DSMs and orthomosaics. We set the processing parameters in Agisoft Metashape® to "high" for photo alignment accuracy and "high" quality and "aggressive" depth filtering for dense point cloud generation. For the details of the photogrammetric survey data and elaboration refer to Table 1.

We generated a 0.2 m/pixel DSM (Fig. 2) and a 0.1 m/pixel orthophotomosaic, covering an area of about 17 km². Unlike a digital elevation model (DEM), the DSM represents the elevation of the highest object within the bounds of a cell. Vegetation, buildings, and other objects have not been removed from the data.

The dataset was processed and analysed in the REGCAN95/UTM zone 28 N [EPSG:4083] Coordinate System. The transformation from ellipsoidal to orthometric heights has been performed using the Geoid model EGM08-REDNAP (https://datos-geodesia.ign.es/geoide/).

Elevation change detection. Elevation change detection (Fig. 3) was obtained by differencing our surveys and a pre-event 2m-pixel DTM acquired in 2015 for the Spanish PNOA-LiDAR project[25]. The assumption is that between the acquisition of the pre-event DTM (2015) and the beginning of the volcanic activity (19 September 2021), no significant height variation took place in the study area, so that elevation differences obtained in our analysis are mainly linked to the volcanic eruption. To subtract the post- and pre-event surveys, we resampled our DSM to 2 m/pixel resolution (same resolution as the 2015 DTM). Considering the vertical Root Mean Square
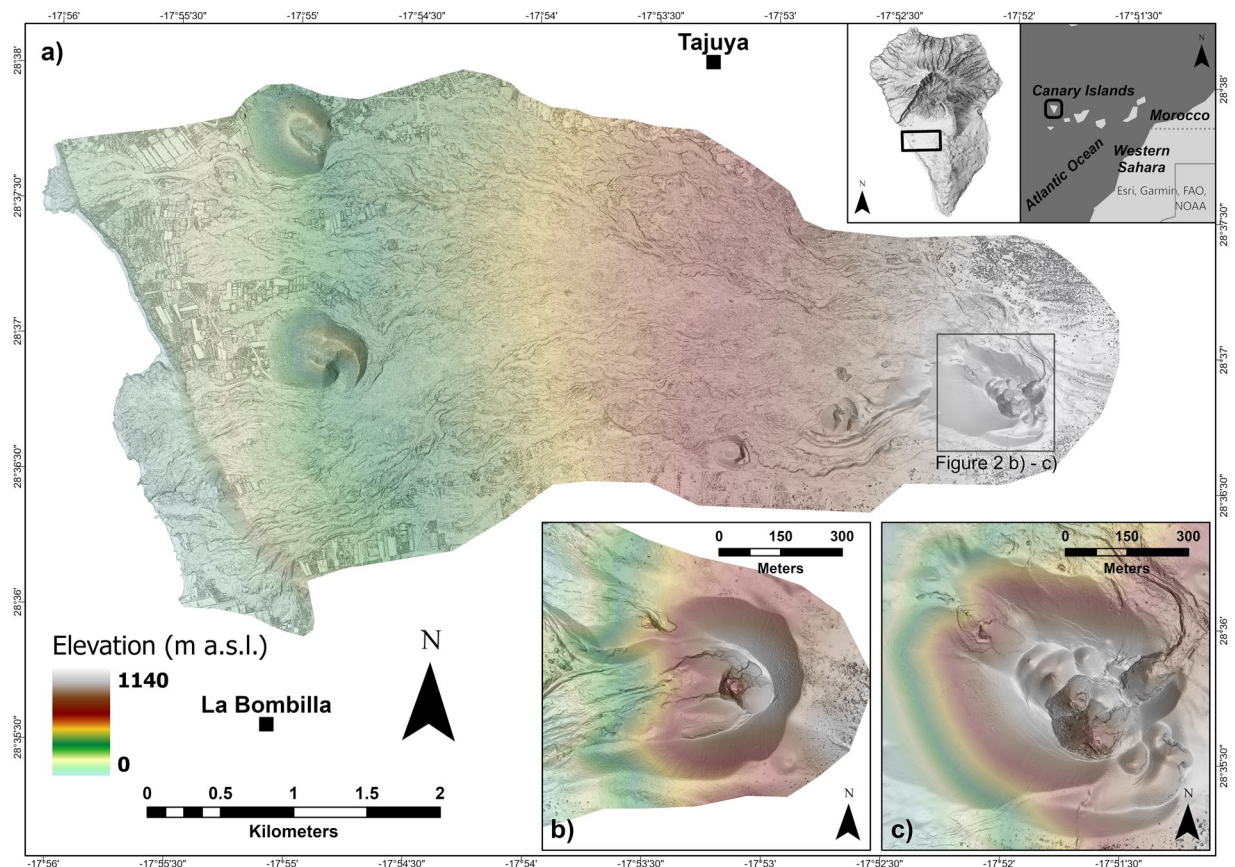
Fig. 2 Digital Surface Model (DSM) of the 2021 eruption deposit of Cumbre Vieja volcano. (**a**) Multidirectional hillshade of the DSM. The inset at the top right of the figure shows the location of La Palma island and the survey area. The grey square in the eastern portion of the study area marks the extent of Fig. 2b,c; (**b**) detailed view of the cone on 27 September 2021[26] and (**c**) in January 2022, respectively.

Error (RMSE) of 0.26 m for our model (before resampling), we set the threshold elevation change (minimum level of detection or minimum elevation change that can confidently be considered a true change) to 0.5 m. It is worth mentioning that the pre-event reference surface is a DTM while our product is a DSM. Such difference must be considered when subtracting both layers as height contributions from vegetation and buildings are still present on the DSM. However, the contribution of such areas is negligible as they are not present above the lava flows and in the cone area.

Data Records

The data record consists of a high-resolution (0.2 m/pixel) photogrammetric Digital Surface Model processed from survey campaign photographs using Agisoft Metashape®. Details of the photogrammetric survey data and elaboration are summarised in Table 1. The Digital Surface Model was processed and analysed in the REGCAN95/UTM zone 28 N [EPSG:4083] Coordinate System. The dataset is stored in GeoTIFF file format in the OpenTopography repository[27] and is shared under the CC BY 4.0 use license.

Technical Validation

Errors in our photogrammetrically-generated DSM result from a complex interplay of geometric and physical parameters, such as image scale, GSD, camera network geometry (nadiral, cross, oblique strips), percentages of image overlap (forward and sidelap), camera shutter speed and exposure settings, lens specifications, image sharpness, camera calibrations, flight design (e.g., flight-line geometry and altitude), surface texture and albedo, lighting conditions, accuracy and distribution of GCPs, disturbances from volcanic activity, as well as on processing: SfM, BBA, image matching, point cloud noise, and outlier removal algorithms.

We therefore applied several strategies to mitigate errors, among which the most important were the following: (1) the use of fast ($>$1/400 s) camera shutter speeds (i.e., exposure times) whenever possible, (2) the variation of flight altitudes and camera orientation, (3) the application of best practices for processing in Agisoft Metashape, (e.g.[12]), and (4) the removal of sparse cloud points with large uncertainty via Metashape's gradual selection tools.

The technical quality of the reconstructed DSM was assessed by using the survey report generated by Agisoft Metashape® and by comparing our DSM to a pre-event DTM[25]. According to the Agisoft Metashape® survey report the GCPs and check points error estimates are as follows: the total GCPs Root Mean Square Error (RMSE)
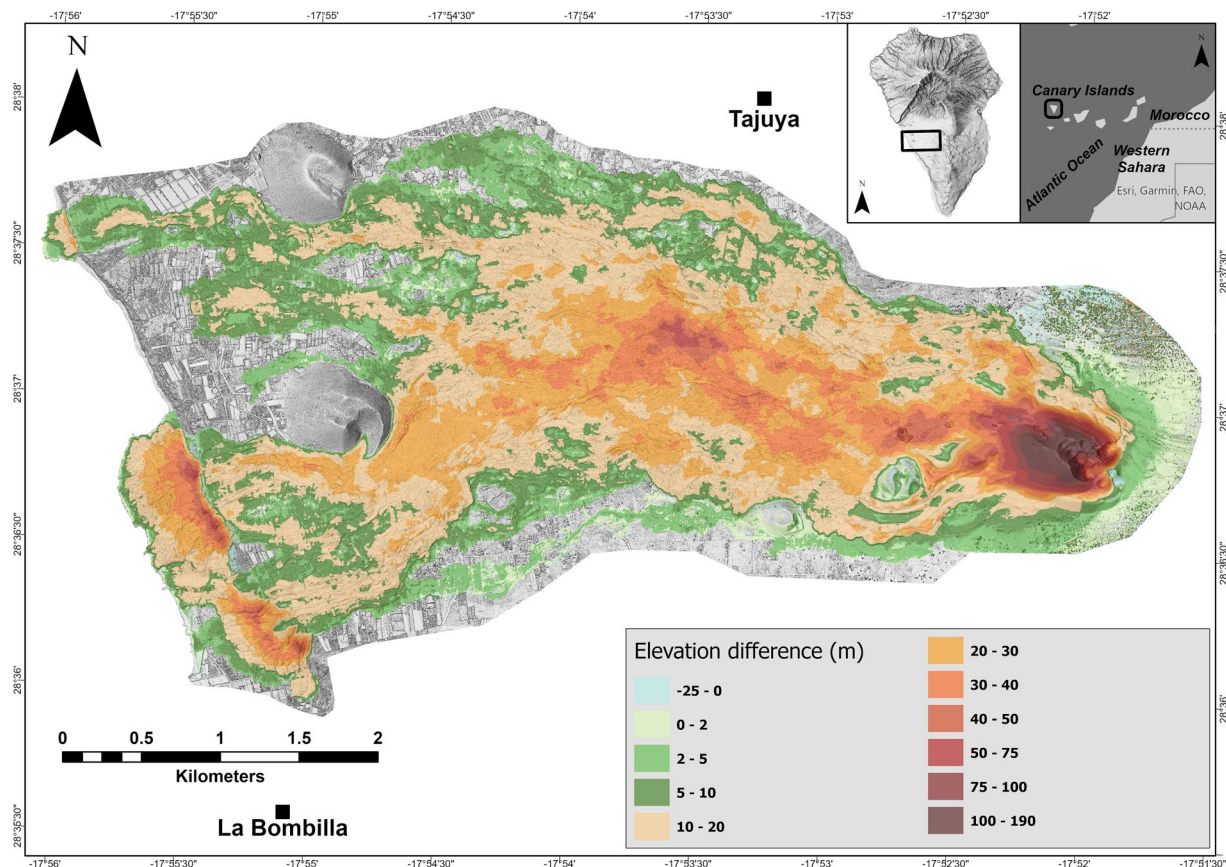
Fig. 3 Elevation difference map for the period 2015 - January 2022 (pre- and post-2021 eruption).

Type	Count	X error (cm)	Y error (cm)	Z error (cm)	XY error (cm)	Total (cm)
Ground control points	33	2.22233	2.93895	4.9619	3.68459	6.18035
Check points	7	8.40241	7.77961	9.0432	11.4509	14.5912

Table 2. Ground control points (GCPs) and check points Root Mean Square Error (RMSE). X - Easting, Y - Northing, Z - Altitude.

is 6.18 cm and the total check points RMSE is 14.59 cm (Table 2). The residual elevation difference with respect to a 2 m/pixel pre-event (2015) DTM[25] extracted at 13 check points placed in the unchanged regions of our DSM was used as an additional indication of the vertical RMSE, which is 0.26 m. Our model is thus sufficiently accurate for the scale of changes reported in this study.

Code availability

No custom code was used to generate or process the data described in the manuscript.

References

1. Carr, B. B., Clarke, A., Arrowsmith, J. R., Vanderkluysen, L. & Dhanu, B. E. The emplacement of the active lava flow at Sinabung Volcano, Sumatra, Indonesia, documented by Structure-from-Motion photogrammetry. *J. Volcanol. Geotherm. Res.* **382**, 164–172, https://doi.org/10.1016/j.jvolgeores.2018.02.004 (2019).
2. Favalli, M. *et al.* Evolution of an active lava flow field using a multitemporal LIDAR acquisition. *J. Geophys. Res. Space Phys.* **115**, 11203, https://doi.org/10.1029/2010JB007463 (2010).
3. James, M. R., Pinkerton, H. & Applegarth, L. J. Detecting the development of active lava flow fields with a very-long-range terrestrial laser scanner and thermal imagery. *Geophys. Res. Lett.* **36**, 22305, https://doi.org/10.1029/2009GL040701 (2009).
4. James, M. & Robson, S. Sequential digital elevation models of active lava flows from ground-based stereo time-lapse imagery. *ISPRS J. Photogramm. Remote Sens.* **97**, 160–170, https://doi.org/10.1016/j.isprsjprs.2014.08.011 (2014).
5. Thiele, S., Varley, N. & James, M. Thermal photogrammetric imaging: A new technique for monitoring dome eruptions. *J. Volcanol. Geotherm. Res.* **337**, 140–145, https://doi.org/10.1016/j.jvolgeores.2017.03.022 (2017).

6. Pallister, J. *et al*. Monitoring, forecasting collapse events, and mapping pyroclastic deposits at Sinabung volcano with satellite imagery. *J. Volcanol.Geotherm. Res.* **382**, 149–163, https://doi.org/10.1016/j.jvolgeores.2018.05.012 (2019).
7. Bisson, M. *et al*. Ten years of volcanic activity at Mt Etna: High-resolution mapping and accurate quantification of the morphological changes by Pleiades and Lidar data. *Int. J. Appl. Earth Obs. Geoinf.* **102**, 102369, https://doi.org/10.1016/j.jag.2021.102369 (2021).
8. Fornaciai, A. *et al*. The 2004–2005 Mt. Etna Compound Lava Flow Field: A Retrospective Analysis by Combining Remote and Field Methods. *J. Geophys. Res. Solid Earth* **126**, 020499, https://doi.org/10.1029/2020JB020499 (2021).
9. Di Traglia, F. *et al*. Joint exploitation of space-borne and groundbased multitemporal InSAR measurements for volcano monitoring: The Stromboli volcano case study. *Remote Sens. Environ.* **260**, 112441, https://doi.org/10.1016/j.rse.2021.112441 (2021).
10. Jordan, B. R. Collecting field data in volcanic landscapes using small UAS (sUAS)/drones. *J. Volcanol. Geotherm. Res.* **385**, 231–241, https://doi.org/10.1016/j.jvolgeores.2019.07.006 (2019).
11. James, M. R. *et al*. Volcanological applications of unoccupied aircraft systems (UAS): Developments, strategies, and future challenges. *Volcanica* **3**, 67–114, https://doi.org/10.30909/vol.03.01.67114 (2020).
12. James, M. & Robson, S. Straightforward reconstruction of 3D surfaces and topography with a camera: Accuracy and geoscience application. *J. Geophys. Res. Space Phys.* **117**, 03017, https://doi.org/10.1029/2011JF002289 (2012).
13. Civico, R. *et al*. Unoccupied Aircraft Systems (UASs) Reveal the Morphological Changes at Stromboli Volcano (Italy) before, between, and after the 3 July and 28 August 2019 Paroxysmal Eruptions. *Remote Sens. 2021* **13**, 2870, https://doi.org/10.3390/rs13152870 (2021).
14. Schmid, M. *et al*. Characterising vent and crater shape changes at Stromboli: Implications for risk areas. *Volcanica* **4**, 87–105, https://doi.org/10.30909/vol.04.01.87105 (2021).
15. De Beni, E., Cantarero, M. & Messina, A. UAVs for volcano monitoring: A new approach applied on an active lava flow on Mt. Etna (Italy), during the 27 February–2 March 2017 eruption. *J. Volcanol. Geotherm. Res.* **369**, 250–262, https://doi.org/10.1016/j.jvolgeores.2018.12.001 (2019).
16. Leggett, T. N., Befus, K. S. & Kenderes, S. Rhyolite lava emplacement dynamics inferred from surface morphology. *J. Volcanol. Geotherm. Res.* **395**, 106850, https://doi.org/10.1016/j.jvolgeores.2020.106850 (2020).
17. Carracedo, J. C., Day, S. J., Guillou, H. & Gravestock, P. Later stages of volcanic evolution of La Palma, Canary Islands: rift evolution, giant landslides, and the genesis of the Caldera de Taburiente. *Geol Soc Am Bull* **111**(5), 755–768, 10.1130/0016-7606(1999)111<0755:LSOVEO>2.3.CO;2 (1999).
18. Fernández, J. *et al*. Detection of volcanic unrest onset in La Palma, Canary Islands, evolution and implications. *Sci Rep* **11**, 2540, https://doi.org/10.1038/s41598-021-82292-3 (2021).
19. Fernández, J., González, P. J., Camacho, A. G., Prieto, J. F. & Brú, G. An Overview of geodetic volcano research in the Canary Islands. *Pure Appl. Geophys.* **172**, 3189–3228, https://doi.org/10.1007/s00445-015-0914-2 (2015).
20. Martí, J., Ortiz, R., Gottsmann, J., Garcia, A. & De La Cruz-Reyna, S. Characterising unrest during the reawakening of the central volcanic complex on Tenerife, Canary Islands, 2004–2005, and implications for assessing hazards and risk mitigation. *J. Volcanol. Geotherm. Res.* **182**, 23–33, https://doi.org/10.1016/j.jvolgeores.2009.01.028 (2009).
21. Martí, J. *et al*. Causes and mechanisms of the 2011–2012 El Hierro (Canary Islands) submarine eruption. *J. Geophys. Res. Solid Earth* **118**, 823–839, https://doi.org/10.1002/jgrb.50087 (2013).
22. Torres-González, P. A. *et al*. Unrest signals after 46 years of quiescence at Cumbre Vieja, La Palma, Canary Islands. *J. Volcanol. Geotherm. Res.* **392**, 106757, https://doi.org/10.1016/j.jvolgeores.2019.106757 (2020).
23. Padrón, E. *et al*. Dynamics of diffuse carbon dioxide emissions from Cumbre Vieja volcano, La Palma, Canary Islands. *Bull. Volcanol.* **77**, 28, https://doi.org/10.1007/s00445-015-0914-2 (2015).
24. PEVOLCA. Informe Comité Científico 25/12/2021: Actualización de la actividad volcánica en Cumbre Vieja (La Palma). https://www3.gobiernodecanarias.org/noticias/wp-content/uploads/2021/12/251221-INFORME-Comité-Científico-PDF.pdf (2021).
25. Centro Nacional de Información Geográfica. Modelo Digital del Terreno - MDT02 https://doi.org/10.7419/162.09.2020.
26. Civico, R. *et al*. 2021 Cumbre Vieja volcano eruption (La Palma, Spain) SfM DSM, Sep 2021, *OpenTopography*, https://doi.org/10.5069/G9R49P0T (2022).
27. Civico, R. *et al*. 2021 Cumbre Vieja volcano eruption (La Palma, Spain) SfM DSM, Jan 2022, *OpenTopography*, https://doi.org/10.5069/G96971S8 (2022).
28. Copernicus Emergency Management Service (© 2021 European Union), [EMSR546] La Palma: Grading Product, Monitoring 63, version 1, release 1, Vector Package https://emergency.copernicus.eu/mapping/ems-product-component/EMSR546_AOI01_GRA_MONIT63_r1_VECTORS/1.

Author contributions
R.C. conceived and designed the work, wrote the original draft, organised the field activities, performed flights and data acquisition/validation, collected the GCPs, curated the datasets and elaborated the photogrammetric data. T.R. conceived and designed the work, wrote the original draft, organised the field activities, performed flights and data acquisition, collected the GCPs, and was responsible for personnel safety, flight authorizations and communications with the air traffic controllers. P.S. supported the work and coordinated the INGV field activities. J.T., D.A. and E.D.B. supported the work and logistics. L.D., P.A.H. and N.M.P. supported the work and coordinated the INVOLCAN/INGV monitoring activities before, during and after the emergency. All Authors reviewed and approved the final version of the manuscript.

Competing interests
The authors declare no competing interests.

Additional information

Correspondence and requests for materials should be addressed to R.C.

Reprints and permissions information is available at www.nature.com/reprints.

Publisher's note Springer Nature remains neutral with regard to jurisdictional claims in published maps and institutional affiliations.